Int. J. Multiphase Flow Vol. 18, No. 2, pp. 295–305, 1992
Printed in Great Britain.

0301-9322/92 $5.00 + 0.00

DISTRIBUTION IN THE VARIOUS TYPES OF PARTICLE TRAJECTORIES NEAR FREELY ROTATING SPHEROIDS IN SIMPLE SHEAR FLOW

J. PETLICKI and T. G. M. VAN DE VEN
Paprican and Department of Chemistry, Pulp and Paper Research Centre, McGill University, Montreal, Canada H3A 2A7

(Received 15 December 1990; in revised form 22 October 1991)

Abstract—In an earlier paper we showed that the relative particle trajectories in simple shear flow of small spheres and large spheroids subjected to attractive van der Waals forces can be divided into five types: (i) trajectories leading to capture of the sphere by the spheroid during the first encounter; (ii) single-pass trajectories; (iii) trajectories leading to capture after successive encounters (transient orbits); (iv) trajectories leading to separation after several transient orbits; and (v) trajectories leading to spheres quasi-chaotically orbiting the spheroid. In this paper we show that the type of trajectory depends on the initial relative position of the sphere and spheroid and the intitial orientation of the spheroid. Using a Monte-Carlo method, we have determined the distribution in the various types of trajectories for various orbit constants and axis ratios of the spheroid.

Key Words: particle deposition, heterocoagulation, two-body hydrodynamic interactions, spheroids in shear flow

INTRODUCTION

In a previous paper (Petlicki & van de Ven 1990) we presented the solution of the trajectory equations for a small but non-Brownian spherical particle near a freely rotating spheroid in simple shear flow. Examples were given of trajectories leading to the capture in primary and secondary energy minima. These interactions show the importance of particle shape in hydrodynamic interactions. The interaction of a small spherical particle with a rotating spheroid is, for example, relevant to papermaking, where small colloidal particles (fillers) interact with pulp fibres which can be modeled as slender spheroids.

Compared with the limiting trajectory approach in the case of two-sphere interactions in simple shear flow (Curtis & Hocking 1970; van de Ven & Mason 1977; Zeichner & Schowalter 1977; van de Ven 1982; Adler 1981a, b), the trajectories of particles in the neighborhood of a spheroid are much more complex. Even if particles cross the same point in the linear flow sufficiently far from the spheroid for the flow field to be undisturbed, the number of possible trajectories is infinite, since an infinite number of spheroid orientations exist relative to a fixed reference frame. In considering the transport of spherical particles to a spheroidal collector in simple shear flow, we have identified by a trial-and-error method five possible states which can be reached by a particle near a spheroidal collector: (i) direct capture; (ii) simple separation; (iii) delayed capture; (iv) delayed separation; and (v) capture in the flow field.

State (i) is reached when a particle is immediately captured by a spheroid during the first encounter. State (ii) is defined by a single-pass trajectory. In cases (iii) and (iv), a particle orbits a spheroid one or more times and in the end is either captured or separates towards infinity. State (v) was employed because in some cases it is impossible to differentiate between states (iii) and (iv) in a reasonable amount of computation time.

In this paper a Monte-Carlo method is used to estimate the probability distributions for the above states as well as the initial distribution of particles captured in a primary energy minimum on the surface of the spheroid.

MONTE-CARLO SIMULATION

Under neutrally buoyant conditions in a Newtonian fluid with viscosity μ, the trajectory of a non-Brownian particle of radius a_p near a spheroidal collector in low Reynolds number simple shear

flow can be found by integrating numerically the following set of dimensionless equations, expressed in a Cartesian frame X (cf. figure 1) rotating with the spheroid:

$$\frac{dx_i}{dt} = F_3 v_i - (F_3 - F_1 F_2)\beta_{2i} \sum_{j=1}^{3} \beta_{2j} v_j + \beta_{2i} \frac{F_1 F_{coll}}{6\pi\mu a_p G b} \quad [1]$$

and

$$\frac{d\psi}{dt} = \frac{1}{2} B \frac{r_e^2 \sin^2\tau - \cos^2\tau}{(r_e^2 \sin^2\tau + \cos^2\tau)[C^2(r_e^2 \sin^2\tau + \cos^2\tau) + 1]^{1/2}}, \quad [2]$$

where

$$\tau = \frac{t}{r_e + r_e^{-1}} + \tan^{-1}\left(\frac{\tan\phi_0}{r_e}\right) \quad [3]$$

and

$$B = \frac{r_e^2 - 1}{r_e^2 + 1},$$

with initial conditions:

for $t = 0$,

$$\phi = \phi_0, x_i = x_{0i} \quad \text{and} \quad \psi = 0.$$

The equatorial semi-axis of the spheroid, b, and the reciprocal shear rate, G^{-1}, have been chosen as the unit length and the unit time, respectively. C is the orbit constant describing the precession of the symmetry axis of the spheroid about the vorticity axis of the undisturbed simple shear flow (figure 1, X'-axis), $r_e = a/b$ is the ratio of the symmetry semi-axis, a, of the spheroid to its equatorial semi-axis, b. β_{2k} are elements of the matrix which transform the local Cartesian coordinate system connected to frame X (rotating with the spheroid) to the frame in which one of the velocity components, v_i, of a fluid element is normal to the surface of the spheroid. F_i are the hydrodynamic correction functions for particle–wall interactions tabulated by Brenner (1961), Goldman *et al.* (1967) and Goren & O'Neil (1971). In the colloidal forces, F_{col}, retarded van der Waals attractions with London wavelength $\lambda_L = 1 \times 10^{-7}$ m (cf. Weise & Healy 1969) were considered so that under these conditions fast deposition occurs. The complete expressions for $v_i = f(r_e, C, \psi, x_i, \tau)$ and β_{ki} are given by Petlicki & van de Ven (1990).

F_i, F_{coll} and β_{2i} are functions of the normal distance between a particle and a spheroid. Although in the rotating frame X the problem of distance is reduced to two dimensions, we were unable to find an analytical solution. Thus, the instantaneous distance was calculated numerically in each integration step. The spin equation [2] gives rise to an elliptic integral with solution $\psi = f(\tau)$ being an oscillating function of time (cf. Hinch & Leal 1979) with frequency depending on the orbit constant, C, and the axis ratio, r_e, of the spheroid. Since the motion of a particle and the rotation of a spheroid are coupled, the system of equations [1, 2] has a stable solution only when the maximal integration step is much smaller than the period of oscillation, regardless of how far the particle is from the spheroid. Obviously, the limitations in the maximal integration step slow down the calculations tremendously when the initial particle position in simple shear flow unperturbed by the spheriod is close to the vorticity plane ($X_1'X_3'$-plane, figure 1), or when a particle orbits the spheroid several times while crossing the vorticity plane far from the spheroid.

The initial orientation of a spheroid relative to a space-fixed Cartesian coordinate system can be expressed (cf. figure 1) in terms of the azimuthal angle, ϕ, which describes the position of the symmetry axis of the spheroid relative to the shear plane and the orbit constant, C. The density of the steady-state orientation distributed function in azimuthal angles, $p_\infty(\phi)$, for an infinite rotary Péclet number ($Pe_r = G/D_r = \infty$, G being the rate of shear and D_r the rotary diffusion coefficient) is known (Anczurowski & Mason 1967) and can be expressed as follows:

$$p_\infty(\phi) = \frac{r_e}{2\pi(r_e^2 \cos^2\phi + \sin^2\phi)}. \quad [4]$$

Thus, in a steady-state a prolate spheroid ($r_e > 1$) spends more time with its symmetry axis aligned along the stream than perpendicular to it. For an oblate spheroid ($r_e < 1$) the opposite is true.

The orbit constant, C, is defined by the following equation:

$$C = \frac{\tan\theta}{r_e}(r_e^2\cos^2\phi + \sin^2\phi)^{1/2}, \qquad [5]$$

where θ is the polar angle. The orbit constant ranges from C = 0 (the symmetry axis perpendicular to the shear plane) to C = ∞ (the symmetry axis in the shear plane).

The steady-state orientation distribution function f(C) in orbit constants was determined by Leal & Hinch (1971) for large but finite Pe_r. Our solution of trajectory equations is exact only for $Pe_r = \infty$ and f(C) is determined solely by the initial distribution of the orbit constants. The Eisenschitz (1932) hypothesis, based on the assumption that particles are initially oriented over all possible directions with equal probability, has never been supported by experiments (cf. Mason & Manley 1956; Anczurowski & Mason 1967). Because of this we performed Monte-Carlo calculations for an orbit constant C = 0, and two arbitrarily chosen orbit constants C = 1 and C$\rightarrow\infty$.

The initial orientation of the spheroid in azimuthal angles, ϕ_0, was selected randomly with weights given by the distribution function, $p_\infty(\phi)$.

The initial positions of the particles were sampled randomly in an arbitrarily chosen plane, perpendicular to the direction of flow and situated in a simple shear flow undisturbed by the spheroid. Because of the symmetry properties of the system (Bretheron 1962), only one quadrant of the $X_1'X_2'$-plane was chosen (cf. figure 1). The plane was divided into a reasonable number of squares (70–150) and in each of them the initial position of a particle was selected randomly. The total number of particles sampled in a given square was in the 50–350 range, depending on the variance analysis of the number of particles intercepted by the spheroid. The calculations were continued until the error in the distribution in the various types of trajectories was $<10\%$. Typically, a quadrant of the capture cross section was sampled up to several thousand times.

For each trial the components of the position vectors of particle were transformed via the appropriate matrix (cf. Petlicki & van de Ven 1990) to frame X, rotating with the spheroid, and the trajectory equations were integrated until we were able to distinguish, at least partially, between states of delayed capture and separation. However, we did not find clear criteria to differentiate trajectories leading to different states in the rotating frame X. Thus, in various time intervals the components of the position vectors were transformed back to frame X' when the criteria are obvious. Since in Jeffery's (1992) solution the disturbance of the velocity field produced by a

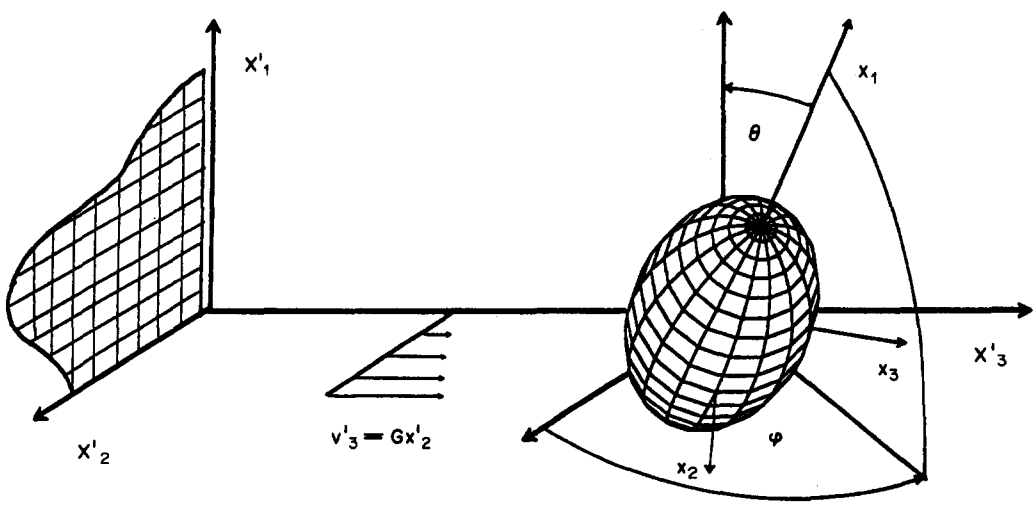

Figure 1. Orientation of a spheroid relative to a space-fixed Cartesian frame X' in simple shear. θ and ϕ are the polar and the azimuthal angles, respectively. Also shown is one quadrant of the capture cross section in the plane $X_1'X_2'$ selected for sampling the initial positions of the particles.

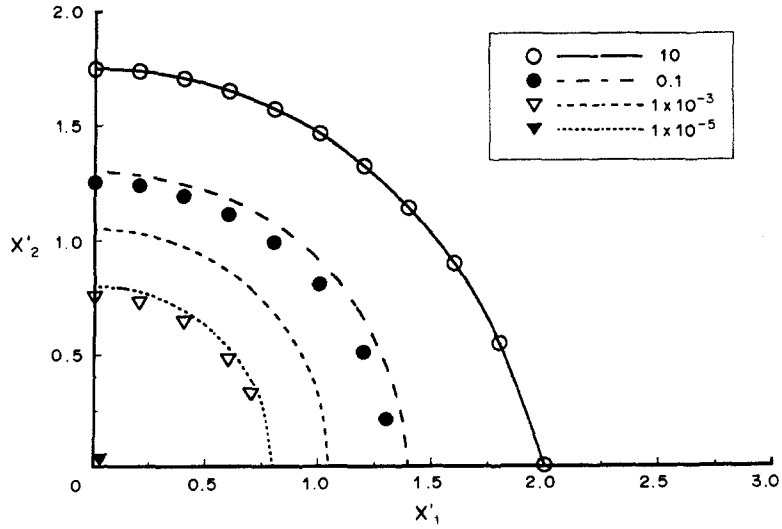

Figure 2. Capture cross sections of two equal spheres as a function of C_A calculated for a retarded attractive force with $\lambda_L/a_p = 0.01$ by Zeichner & Schowalter (1977) (lines) and from [1] and [2] (symbols). The length scale is normalized by the radius of the sphere, a_p.

spheroid decays very slowly, the separation between a sphere and a spheroid was assumed to occur when the distances were >10 major semi-axis of the spheroid.

The surface area of a capture cross section for two spheres in simple shear flow decreases substantially (van de Ven & Mason 1977; Zeichner & Schowalter 1977) when the parameter $C_A = A/6\pi\mu a_p^3 G$ (A and a_p are the Hamaker constant and radius of the sphere, respectively), being a measure of the ratio of colloidal to hydrodynamic forces, decreases. For two non-equal spheres the surface area of capture cross sections (cf. Adler 1981a) decreases very rapidly when the radius ratio of spheres deviates from unity. After several thousands of trials we recognized that the calculation of a capture cross sections requires an unrealistic amount of computer time when colloidal forces are weak and the particle is very small compared with the spheroid.

For sufficiently strong attractive colloidal forces, as has been shown by Dabros & Adamczyk (1979), the increase in the hydrodynamic drag a particle experiences while approaching a solid wall is balanced by the attractive dispersion forces. Fortunately, we found that the effect of the collector curvature on the particles trajectories depends on the ratio of colloidal to hydrodynamic forces, C_A. Figure 2 shows a comparison of the capture cross sections of two equal spheres as a function of C_A, as calculated by Zeichner & Schowalter (1977) and from [1] and [2] with $r_e = 1$. Since capture cross sections are almost the same up to $C_A = 0.1$, we can conclude that the effect of the curvature of spheroidal collectors is negligible for $C_A > 0.1$, even if it equals the curvature of the particle. Thus, for strong enough attractive colloidal forces the size of a particle is only limited by the fact that a large particle can significantly perturb the rotational motion of the spheroid.

RESULTS AND DISCUSSION

The probability density presented in this paper is proportional to the density of points on the graphs, representing the initial positions in the $X_1'X_2'$-plane. The unit length is always the equatorial semi-axis of the spheroid, b. Since the computation time of the first part of a particle trajectory is strongly affected by the relative velocity between the spheroid and the particle, the initial positions of particles with $X_2' = 0.05b$ were usually omitted in the Monte-Carlo calculations.

The probabilities and distribution of states (direct capture, delayed capture and capture in the flow field) for an axis ratio of the spheroid $r_e = 2$ and orbit constant $C = 0$ are shown in figure 3. The probability density for the direct capture state is equal to one. The boundary of the capture cross section is sharp and is defined by the states of delayed capture and capture in the flow field. The probability of delayed separation is equal to zero. Thus, for this particular orbit constant the

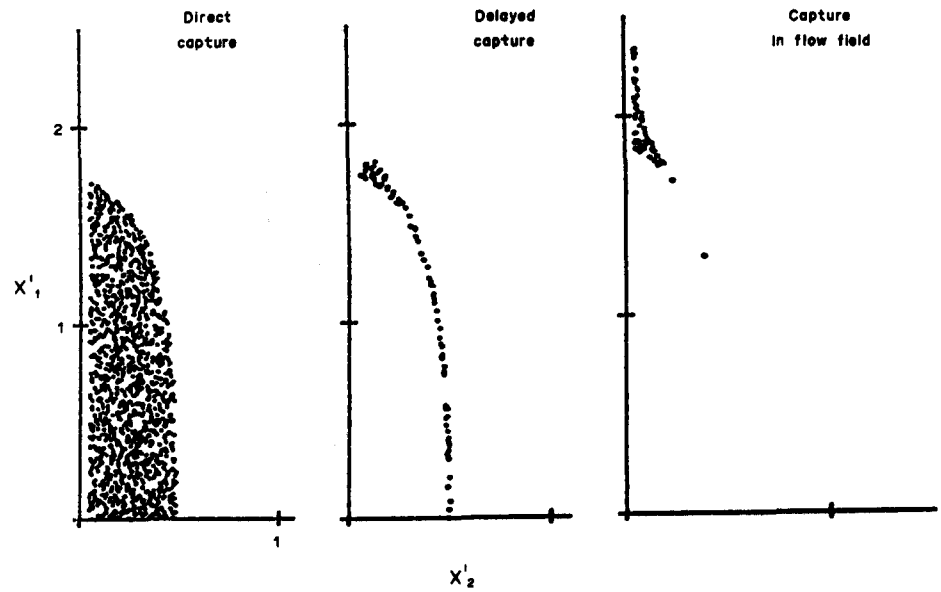

Figure 3. Distribution of states for one quadrant of the capture cross section for $C = 0$ and $r_e = 2$. The length scale is normalized by the equatorial semi-axis of the spheroid $b = 5\,\mu$m. The remaining conditions are: $a_p/b = 0.2$ and $C_A = A/6\pi\mu G a_a b^2 = 1.06$. The probability density is normalized to 50 points/$2.25 \times 10^{-2} b^2$.

solution of the trajectory equations leads to qualitatively the same capture cross sections as for two-sphere interactions in simple shear flow.

Although the capture cross section was computed by using [1] and [2] the problem can be solved more efficiently in frame X'. As was pointed out previously (Petlicki & van de Ven 1990) for $C = 0$ the flow field about the spheroid becomes simplified and for an axis ratio $r_e = 1$ is the same as that given by Cox *et al.* (1968) for a sphere. Additionally, similar to two spheres, it is sufficient to sample points around the boundary of the capture cross section, which speeds up the calculations tremendously.

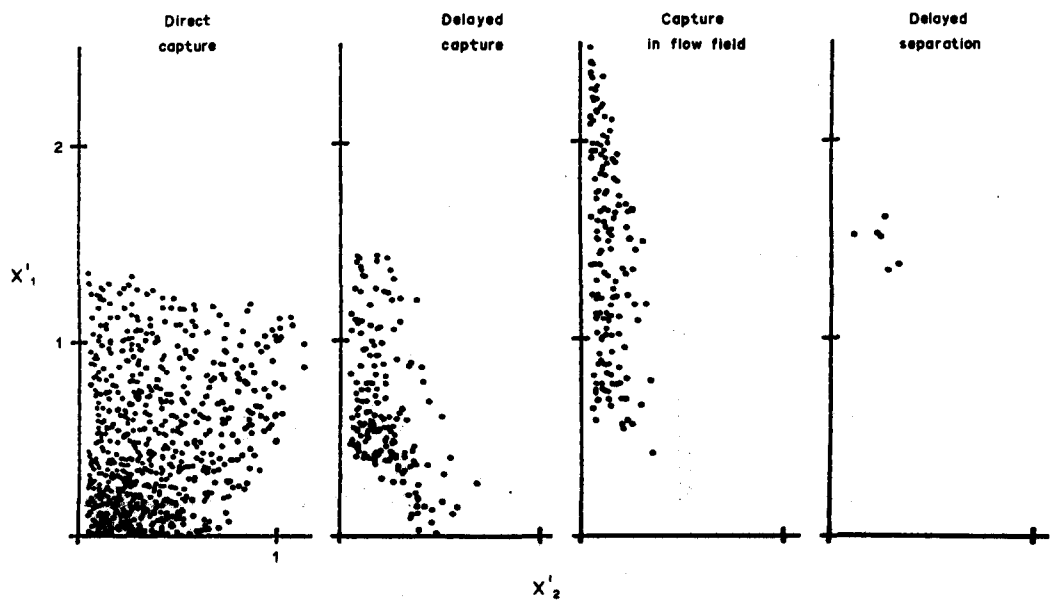

Figure 4. Distribution of states for one quadrant of the capture cross section for $C = 1$ and $r_e = 2$. The remaining parameters are as in figure 3.

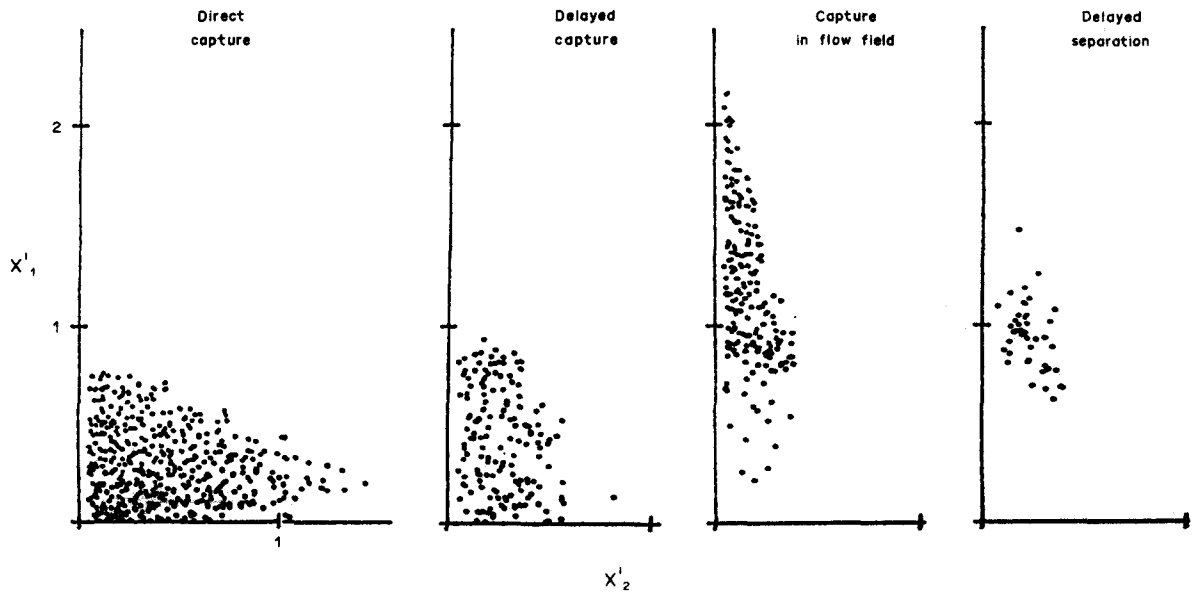

Figure 5. Distribution of states for one quadrant of the capture cross section for $C = 10^5$ and $r_e = 2$. The remaining parameters are as in figure 3.

For the same axis ratio $r_e = 2$, but orbit constants $C = 1$ and $C = 10^5$, the density and distribution of states changes drastically (cf. figures 4 and 5). The delayed separation state appears and all states partially overlap. The probability density of direct capture decreases. In figure 4 there appears to be a region where the probability of direct capture is one, while this region has almost disappeared in figure 5. The boundary of this region is difficult to pinpoint since it is difficult to rule out small probabilities of delayed capture. Figure 6 shows two capture cross sections calculated for the same particle–spheriod system and the same orbit constant, but with the first one computed with the same assumptions as made by Smoluchowski (1917). He approximated two-sphere collisions in simple shear flow by neglecting colloidal and hydrodynamic interactions and with the

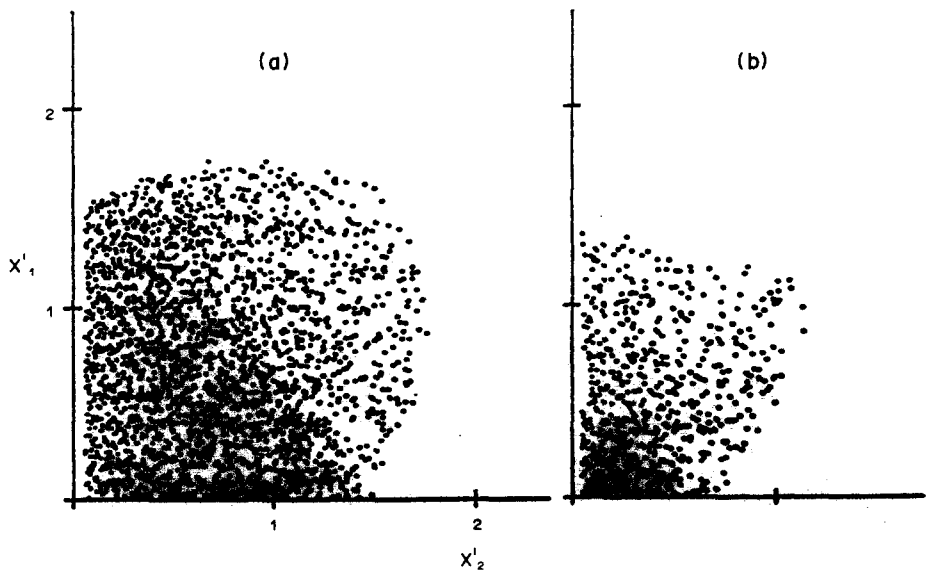

Figure 6. Distribution of the direct capture state for one quadrant of the capture cross section, calculated using the Smoluchowski (1917) approximation (a) and from the full model (b) for $C = 1$ and $r_e = 2$. The remaining parameters are as in figure 3.

undisturbed simple shear flow extended up to the surface of the collision sphere. The collision cross section of a spheroid of semi-axes a and b is one with semi-axes $(a + a_p)$ and $(b + a_p)$. It can be seen that the probability distributions in the plane of the capture cross section are similar and reflect the fact that the projected area of a spheroid in simple shear on the $X_1'X_2'$-plane is a periodic function of time (van de Ven 1989), and the probability of a particle hitting the surface of a spheriod increases in the direction toward the center of the spheroid. Nevertheless, the motion of a particle and the rotation of the spheroid are coupled and the local value of the probability density depends on the selection of the reference plane ($X_1'X_2'$-plane in figure 1). However, it was found that the number of collisions between spheres and spheroids is practically independent of the choice of the location of the reference plane.

As was mentioned above, the state of capture in the flow field was introduced because we were unable to distinguish between the delayed capture state and the delayed separation state in a reasonable amount of computation time. For an orbit constant $C = 0$, the situation is clear since the delayed capture state does not exist. All particles crossing the limiting trajectory under the action of attractive colloidal forces have to be captured sooner or later. For $C > 0$, the trajectories leading to capture in the flow field are distributed in between those leading to delayed capture and delayed separation, depending on the orbit constant and the axis ratio of the spheroid.

Figures 7, 4, 8 and 9 show the results for $C = 1$ and $r_e = 5$, 2, 0.5 and 0.2, respectively. Although a comparison of spheroids rotating with the same orbit constant and different axis ratios is risky because they rotate completely differently (cf. [5]), the relative density of the delayed separation and capture state increases as the period of rotation of a spheroid $T = 2\pi(r_e + r_e^{-1})G^{-1}$ increases.

The initial number of collisions per spheroid can be calculated in the same way as for two-sphere interactions (van de Ven & Mason 1977). The contribution of a characteristic tail in the capture cross section for the particle capture in the flow field (cf. figure 3) is not important for $C = 0$ and strong colloidal interactions, since particle velocities are relatively small in this region of the capture cross section. For orbit constants $C > 0$, the contribution of trajectories leading to capture in the flow field, as well as leading to delayed capture, can be substantial and the initial number of collisions per spheroid can be estimated only with limited accuracy.

Figures 8 and 10 show the influence of the ratio of colloidal forces to the hydrodynamic forces C_A and the size of the particle on the capture cross sections of disks with axis ratio $r_e = 0.5$ rotating

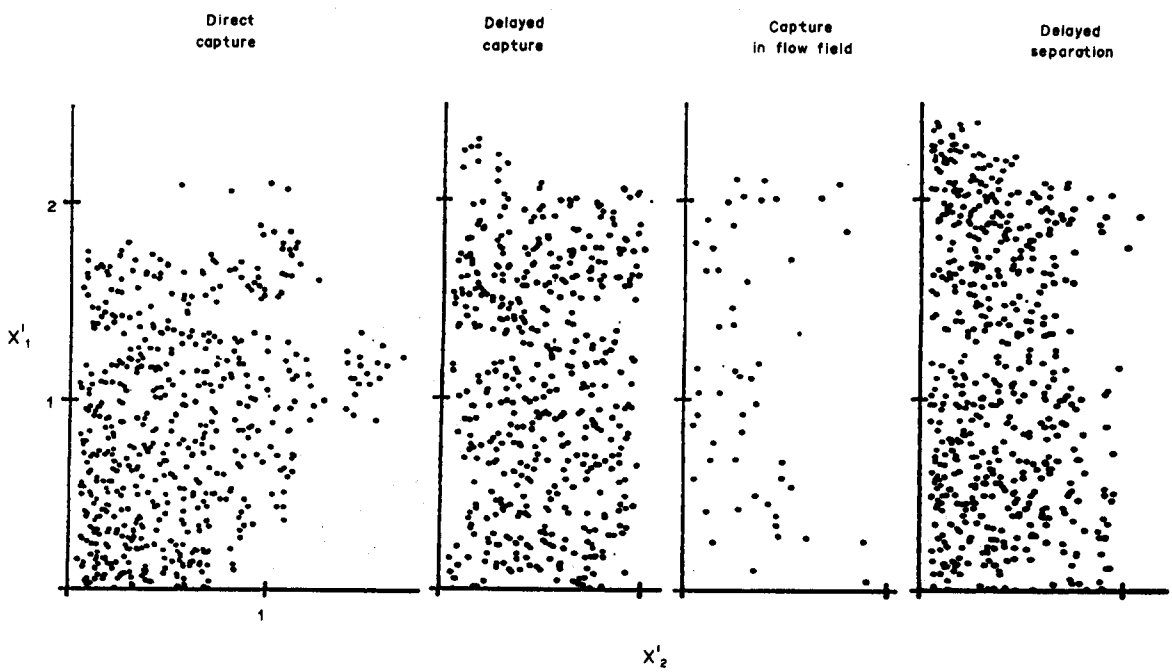

Figure 7. Distribution of states for one quadrant of the capture cross section for $C = 1$ and $r_e = 5$. The remaining parameters as in figure 3.

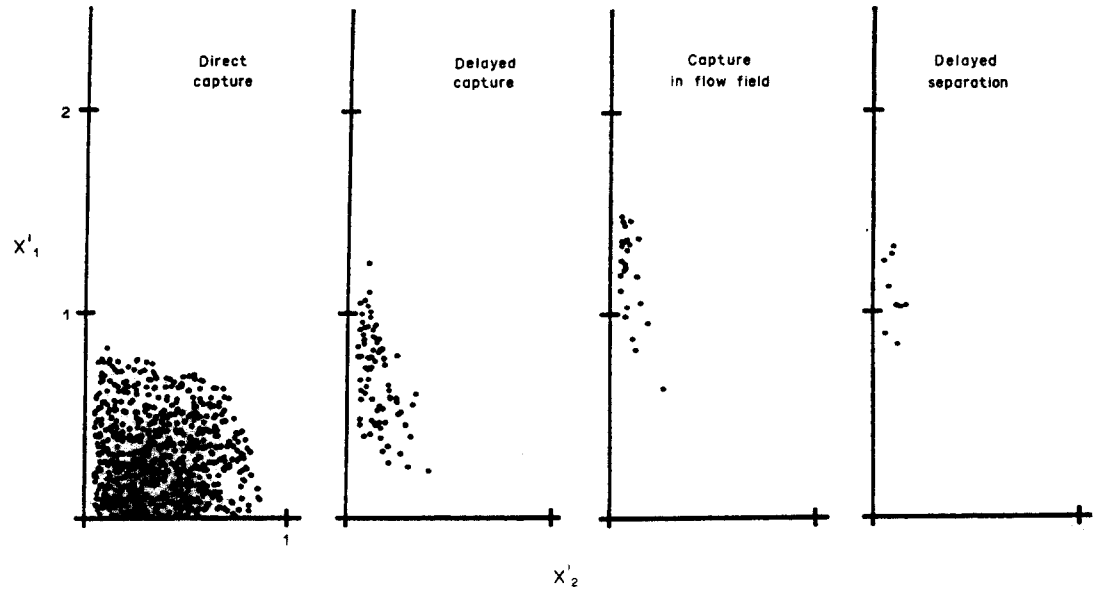

Figure 8. Distribution of states for one quadrant of the capture cross section for C = 1 and $r_e = 0.5$. The remaining parameters as in figure 3.

with orbit constant C = 1. The calculation of the data in figure 10 was performed on a computer about 20 times faster than the one used in calculating figure 8. In order to distinguish between states of delayed capture and separation, the computation time for each trajectory was about 4 times longer than that of figure 8. The probability of direct capture is about 2 orders of magnitude lower. The area of the capture cross section occupied by the state of direct capture decreases but its "shape" does not change. The distributions of delayed capture, separation and capture in flow field states are similar to those in figure 8, but the relative probability of those states is much higher.

Similar to two spheres, the capture efficiency (van de Ven & Mason 1977) can be introduced as the ratio of the number of collisions estimated from the full model and the number obtained using

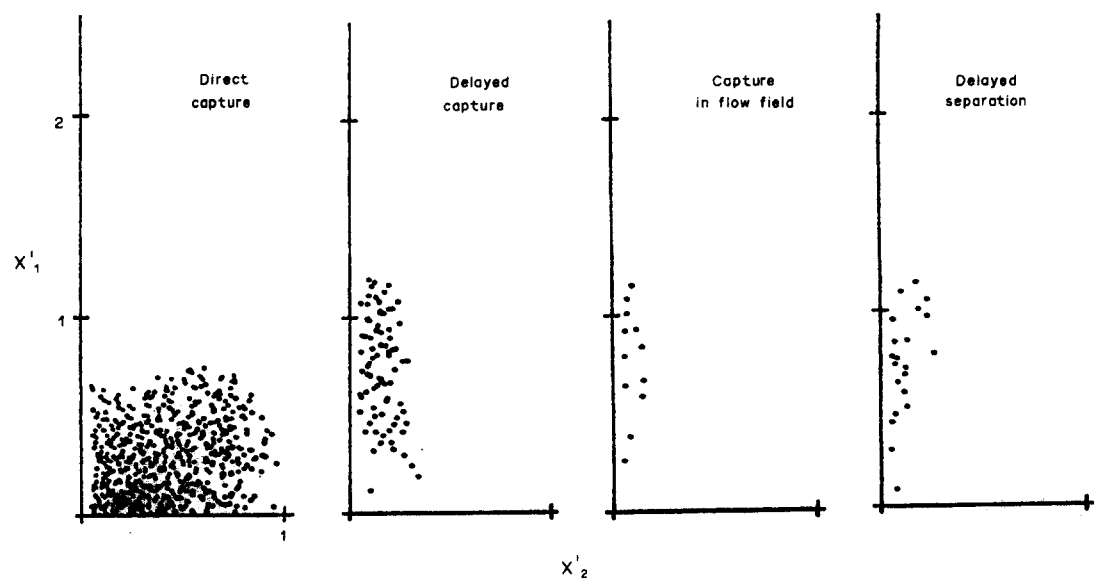

Figure 9. Distribution of states for one quadrant of the capture cross section for C = 1 and $r_e = 0.2$. The remaining parameters as in figure 3.

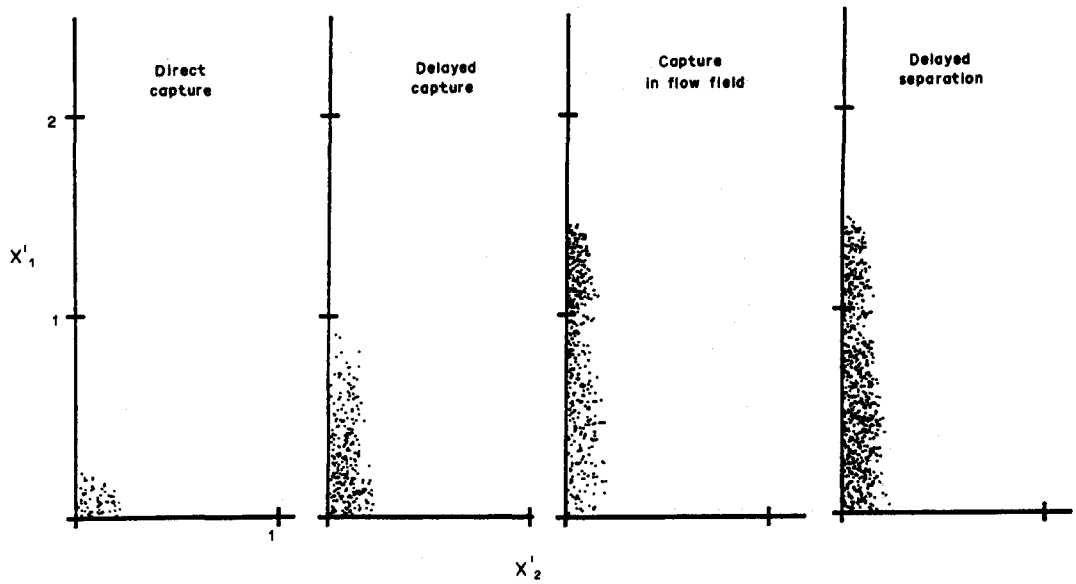

Figure 10. Distribution of states for one quadrant of the capture cross section for C = 1 and $r_e = 0.5$. The remaining parameters are: $b = 20\,\mu$m, $a_p/b = 0.1$, $C_A = A/6\pi\mu a_p b^2 = 3.32 \times 10^{-3}$.

the Smoluchowski (1917) approximation (cf. figure 6). However, first the problem of the dependency of the Smoluchowski approximation on the orbit constant and axis ratio of the spheroid must be solved and the influence of the initial distribution of the orbit constants on the initial number of collisions has to be estimated.

Figure 11 shows the initial distribution of particles captured on the surface of a spheroid as a function of orbit constant. The distributions were projected on both the X_1X_2- and X_1X_3-planes and averaged. For orbit constants close to zero the distribution is uniform along the symmetry axis except at the poles where deposition is restricted by weak colloidal interactions. When the orbit constant increases, particles are deposited near the poles of the prolate spheroid rather than near its equator. For disk-like particles the probability of capture increases in the direction of the edges of the spheroid. Thus, in a dilute suspension containing an insufficient number of particles to obtain a full coating of the surfaces of the spheroids, a non-uniform coverage of particles on the spheroids should occur.

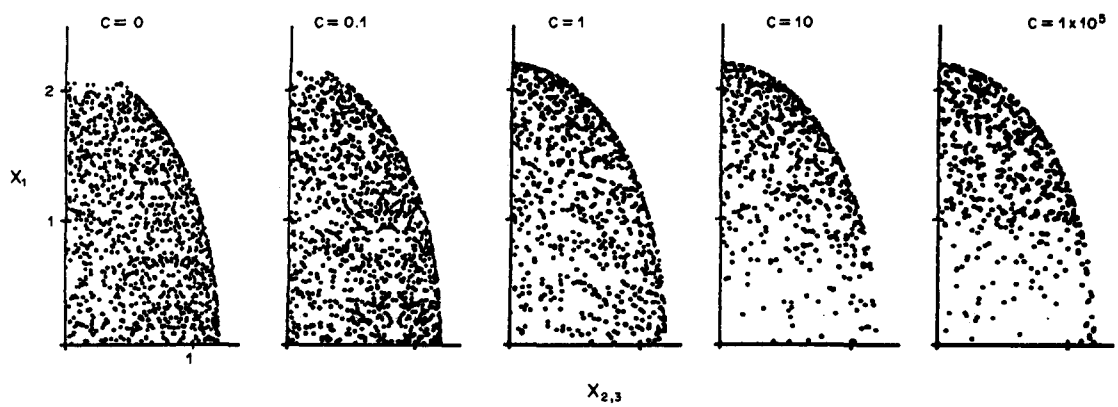

Fig. 11. Initial particle distribution on the surface of the spheriod (one quadrant) in the projection on the X_1–X_2X_3 plane (in particle-fixed coordinates) for $r_e = 2$.

CONCLUDING REMARKS

In this paper we took the first step in quantifying the number of collisions between spherical particles and spheroidal collectors freely rotating in simple shear flow. Compared to two-sphere interactions, the problem is, in general, much more complex. Two additional parameters play a role in the process of heterocoagulation: the orbit constant and the axis ratio of the spheriod. The influence of the orbit constant is crucial because in the sphere–spheroid systems under consideration the initial distribution of the orbit constants is usually unknown.

It was shown that the trajectories between attractive spheres and spheroids can be divided into five types, two of which result in contact between the particles, i.e. on deposition of the sphere on the spheroid. The distribution of the deposited particles was found to be non-uniform and to depend on the orbit constant and axis ratio of the spheriod.

Acknowledgement—This work was supported by the Natural Science and Engineering Council of Canada through Strategic Grant No. G1677.

REFERENCES

ADLER, P. M. 1981a Heterocoagulation in shear flow. *J. Colloid Interface Sci.* **83,** 106–115.

ADLER, P. M. 1981b Interaction of unequal spheres. I. Hydrodynamic interaction: colloidal forces. *J. Colloid Interface Sci.* **84,** 461–474.

ANCZUROWSKI, E. & MASON, S. G. 1967 The kinetics of flowing dispersions. II, III. Equilibrium orientations of rods and discs. *J. Colloid Interface Sci.* **23,** 522–546.

BRENNER, H. 1961 The slow motion of a sphere through a viscous fluid towards a plane surface. *Chem. Engng Sci.* **16,** 242–251.

BRETHERTON, F. P. 1962 The motion of rigid particles in a shear flow at low Reynolds number. *J. Fluid Mech.* **14,** 284–304.

CURTIS, A. S. G. & HOCKING, L. M. 1970 Collision efficiency of equal spherical particles in a shear flow. *Trans. Faraday Soc.* **66,** 1381–1390.

COX, R. G., ZIA, I. Y. Z. & MASON, S. G. 1968 Particle motions in sheared suspensions. XXV. Streamlines around cylinders and spheres. *J. Colloid Interface Sci.* **27,** 7–18.

DABROS, T. & ADAMCZYK, Z. 1979 Noninertial particle transfer to the rotating disk under an external force field. *Chem. Engng Sci.* **34,** 1041–1049.

EISENSCHITZ, R. 1932 Die Viscosität von Suspensionen langgestreckter Teilchen und ihre Interpretation durch Raumbeanspruchung. *Z. Phys. Chem.* **A158,** 78–90.

GOLDMAN, A. J., COX, R. G. & BRENNER, H. 1967 Slow motion of a sphere parallel to a plane wall. Part I. Motion through a quiescent liquid. Part II. Couette flow. *Chem. Engng Sci.* **22,** 637–652; 653–600.

GOREN, S. L. & O'NEILL, M. E. 1971 On the hydrodynamic resistance to a particle of a dilute suspension when in the neighbourhood of a large obstacle. *Chem. Engng Sci.* **26,** 325–388.

HINCH, E. J. & LEAL, L. G. 1979 Rotation of small non-axisymmetric particles in a simple shear flow. *J. Fluid Mech.* **22,** 591–608.

JEFFERY, G. B. 1922 The motion of ellipsoidal particles immersed in a viscous fluid. *Proc. R. Soc. Lond.* **A102,** 161–179.

LEAL, L. G. & HINCH, E. J. 1971 The effect of weak Brownian rotations on particles in shear flow. *J. Fluid Mech.* **46,** 685–703.

MASON, S. G. & MANLEY, R. St. J. 1956 Particle motions in sheared suspension: orientations and interactions of rigid rods. *Proc. R. Soc. Lond.* **A238,** 117–131.

PETLICKI, J. & VAN DE VEN, T. G. M. 1990 Particle trajectories near freely rotating spheroids in simple shear flow. *Int. J. Multiphase Flow* **16,** 713–725.

SMOLUCHOWSKI, M. 1917 Versuch einer mathematischen Theorie der Koagulationskinetik kolloider Lösungen. *Z. Phys. Chem.* **92,** 129–168.

VAN DE VEN, T. G. M. 1982 Interactions between colloidal particles in simple shear flow. *Adv. Colloid Interface Sci.* **17,** 105–127.

VAN DE VEN, T. G. M. 1989 *Colloidal Hydrodynamics*, p. 246. Academic Press, New York.

VAN DE VEN, T. G. M. & MASON, S. G. 1977 The microrheology of colloidal dispersions. VII. Orthokinetic doublet formation of spheres. *Colloid Polym. Sci.* **255,** 468–479.

WEISE, G. R. & HEALY, T. W. 1969 Effects of particle size on colloid stability. *Trans. Faraday Soc.* **66,** 490–499.

ZEICHNER, G. R. & SCHOWALTER, W. R. 1977 Use of trajectory analysis to study stability of colloidal dispersions in flow fields. *AIChE Jl* **23,** 243–254.